THE UNIVERSITY OF ALBERTA

RELEASE FORM

NAME OF AUTHOR....Keith Roger Betty, B.Sc.

TITLE OF THESIS..A Secondary Battery based on the

...Copper(II)-(I) and Copper(I)-(0) Couples

...in Acetonitrile

DEGREE FOR WHICH THESIS WAS PRESENTED..M.Sc.

YEAR THIS DEGREE GRANTED...1973

Permission is hereby granted to THE UNIVERSITY OF ALBERTA LIBRARY to reproduce single copies of this thesis and to lend or sell such copies for private, scholarly or scientific research purposes only.

The author reserves other publication rights, and neither the thesis nor extensive extracts from it may be printed or otherwise reproduced without the author's written permission.

G. S.

THE UNIVERSITY OF ALBERTA

A SECONDARY BATTERY BASED ON THE COPPER(II)-(I) AND COPPER(I)-(0) COUPLES IN ACETONITRILE

by

© KEITH ROGER BETTY

A THESIS

SUBMITTED TO THE FACULTY OF GRADUATE STUDIES AND
RESEARCH IN PARTIAL FULFILMENT OF THE REQUIREMENTS
FOR THE DEGREE OF MASTER OF SCIENCE

DEPARTMENT OF CHEMISTRY

EDMONTON, ALBERTA

FALL, 1973

THE UNIVERSITY OF ALBERTA

FACULTY OF GRADUATE STUDIES AND RESEARCH

The undersigned certify that they have read, and recommend to the Faculty of Graduate Studies and Research, for acceptance, a thesis entitled ...A...... Secondary Battery Based on the Copper(II)-(I) and .... Copper(I)-(0) Couples in Acetonitrile .... submitted by...Keith Roger Betty...................... in partial fulfilment of the requirements for the degree of Master of Science in Analytical Chemistry.

ABSTRACT

A secondary cell based on the copper(II)-(I) and copper(I)-(0) couples in acetonitrile has been constructed and studied. A cathode compartment consisting of a graphite sheet in contact with an acetonitrile solution of copper(II) perchlorate was separated by an anionic ion-exchange membrane from an anode compartment consisting of copper wire in contact with an acetonitrile solution of lithium or sodium perchlorate. The discharge product at each electrode is copper(I) perchlorate. The cell has a practical voltage of 1.35 v, and is reversible; a test unit was carried through more than 45 charge and discharge cycles.

The proposed system possesses voltage and current efficiencies comparable to those of commercial lead-acid and nickel-cadmium cells. Energy density of the experimental battery is low, primarily due to the weight of structural components. However, the theoretical energy density of 50 W-hr/lb is also low, about half that lead-acid and nickel-cadmium batteries, due to both the low voltage of the experimental cell and the high equivalent weight of $Cu(ClO_4)_2$ (262). Studies of battery performance indicate that cell performance diminishes considerably when the temperature is lowered from 25°C to -14°C.

An anionic ion-exchange membrane was used to separate the anodic and cathodic compartments of the

battery. The membrane was found to be stable to the solvent, chemicals, and potentials used, and it effectively blocks transport of copper(II) species. A cell retained 88% of full charge after two months wet stand.

ACKNOWLEDGEMENTS

The author would like to express his appreciation to John Senne and Eric Grimsrud for help in purification of chemicals; to G. Horlick for the loan of equipment; to Lavine Straub who did the typing and to Glen Johanson for preparation of the illustrations; and especially to Dr. B. Kratochvil for his understanding and assistance.

Financial support from the University of Alberta and the National Research Council of Canada is gratefully acknowledged.

TABLE OF CONTENTS

CHAPTER PAGE

LIST OF TABLES

LIST OF FIGURES

Figure Page

I

INTRODUCTION

Batteries may be divided into two major types. The primary battery, of which the best example is the dry cell, is designed to be used once and discarded. The secondary battery, of which the best example is the lead-acid storage battery, may be recharged and therefore re-used. The chemical and physical requirements of the secondary battery are necessarily much more stringent than those of the primary battery.

Much work is being done at the present time to develop new battery systems. Most of this work centers around high-energy density systems that may be used as power sources in vehicles or for applications in space travel. However, relatively little work is being done towards the development of batteries that can function efficiently at low ambient temperatures. Such a system, if developed, could be used as a stationary power source for arctic and sub-arctic installations. It was with this eventual goal in mind, and to learn more about the behaviour of the copper couples in acetonitrile, that the present work was conducted.

An aqueous battery system is obviously unsuitable for ambient operation in the sub-zero temperatures commonly found in high latitudes. It is therefore necessary to

search for a non-aqueous solvent with desirable properties. Such a solvent should have a low freezing point, readily solvate ionic species, possess a low viscosity to facilitate ion transport, and be stable towards electrochemical oxidations or reductions. It should also be cheap and readily available. In Table I are listed some physical properties of four organic solvents.[1] It can be seen that acetonitrile (AN) satisfies many of the requirements given above.

Acetonitrile is a polar Lewis base,[2] and, although it solvates cations moderately well, it is a poor solvator of anions. Therefore, the salts of highest solubility are those having large symmetrical or polarizable univalent anions such as perchlorate, in which the charge density on the anion is low. The stability of acetonitrile towards electrochemical oxidation or reduction is quite high. The useful potential range extends from +2.2 v to -3.1 v versus the Ag/0.01 $\underline{M}$ $AgNO_3$ electrode in acetonitrile.[1]

Methods of purification for acetonitrile have been studied exhaustively by Coetzee.[3] The pure solvent takes up water readily, and special precautions are required to keep water concentrations below millimolar levels. The toxicity[4] is moderate due to slow hydrolysis in the body to cyanide, but is much lower than that of many

Table I

Physical Properties of Selected Solvents [1]

	Acetonitrile (AN)	Dimethyl-sulfoxide (DMSO)	Propylene carbonate (PC)	Dimethyl-formamide (DMF)
Dielectric constant	36.0	46.7	69.0	36.7
Boiling Point, °C	82	189	242	153
Melting Point, °C	-45	18	-40	-6
Density, gm/cm^3	0.777	1.101	1.206	0.944
Viscosity, cP	0.35	1.99	2.52 [10]	0.80
Dipole moment, Debye	3.37	4.3	4.98	3.82
Specific conductivity, [19] ohm^{-1} cm^{-1}	10^{-7} to $7x10^{-6}$	$2x10^{-8}$ to $0.87x10^{-7}$	$1.0x10^{-7}$ to $2x10^{-7}$	10^{-7} to $1.2x10^{-6}$
Useful potential range	+2.2 to -3.1 v vs Ag/0.01 M $AgNO_3$ in AN	+1.0 to -3.0 v vs SCE (aq)[20]	+3.2 to -4.1 v vs Ag/0.01 M $AgNO_3$ in PC[21]	+1.4 to -3.8 v vs Hg/Hg_2^{2+}(31)

other common organic solvents such as glacial acetic acid. Precautions should be taken, however, to minimize exposure to both the vapor and the liquid.

The feasibility of using acetonitrile as a solvent for a low-temperature battery has been investigated.[5] Dry cells of the type

$$\mathrm{Zn}|\mathrm{AN},\mathrm{NH_4SCN}|\mathrm{MnO_2},\mathrm{C}$$

have been studied,[6] and found to perform considerably better than a conventional "D" dry cell at -42°C. Solomon[7] developed a battery utilizing a calcium negative and a silver chloride positive in the solvent mixture acetonitrile-propionitrile that would function effectively at temperatures as low as -100°F. He does not, however, specify the electrolytes.

The cell chosen for investigation in this work may be represented schematically as

$$\mathrm{Cu}|\mathrm{AN},\mathrm{MClO_4}||\mathrm{Cu(ClO_4)_2},\mathrm{AN}|\mathrm{C},$$
$$\text{where } M = Li^+,\ Na^+$$

The cathodic reaction is

$$Cu^{2+} + e^- \rightarrow Cu^+$$
$$E° = +0.679 \text{ v vs std Ag electrode}^{12}$$

and the anodic reaction is

$$Cu° \rightarrow Cu^{+} + e^{-}$$

$$E° = +0.6044 \text{ v vs std Ag electrode}^{12}$$
$$\text{(as oxidation)}$$

The appreciable difference in the potentials of the two couples in acetonitrile compared to water is caused by the strong solvation of copper(I) relative to copper(II) by this solvent.

For practical use of the cell described above, it is necessary to prevent migration of copper(II) to the anode where it will react with copper metal, resulting in self-discharge of the battery. An anionic ion-exchange membrane was therefore inserted between the anodic and cathodic compartments. Solutions of 0.75 $\underline{M}$ $LiClO_4$ [8] and 0.8 $\underline{M}$ $NaClO_4$ [9] in acetonitrile have both been found to possess a relatively high specific conductance of 3×10^{-2} ohm^{-1} cm^{-1}, indicating that either would be suitable as supporting electrolyte. Further, association of these salts is not great, the ion pair association constants being 4 for $LiClO_4$ and 10 for $NaClO_4$.[10] The proposed system possesses the inherent simplicity that both anodic and cathodic discharge reactions produce the same product - a simplicity shared by the lead-acid battery.

The Cu(I)-Cu(O) and Cu(II)-Cu(I) couples in

acetonitrile have been investigated by several workers.[11-17] Voltammetric studies at a platinum electrode indicate that the Cu(II)-Cu(I) couple is reversible.[13] Manahan,[14] using radiotracer techniques, estimated a minimum value of the rate constant *k* for electron transfer of 0.3 F^{-1} sec^{-1}, assuming first order kinetics in both Cu(II) and Cu(I). In a chronopotentiometric study, Kowalski and Lingane[15] found that electron exchange between copper(I) and hydrated copper(II) at a platinum electrode was quasireversible. Similar results were obtained by McDuffie[16] using thin-layer steady-state voltammetry. Biallozor[17] found that electrodeposition of copper on platinum from acetonitrile solution was irreversible, but with a relatively low overpotential. Table II gives the standard potentials at 25° of the Cu(II)-Cu(I) and Cu(I)-Cu(O) couples, along with potentials of the silver couple under several conditions.[12]

Several discharge and recharge methods may be used to cycle a cell.[18] The best discharge method from the standpoint of convenience of instrumentation is discharge through a constant resistance. However, information on electrochemical behaviour is difficult to extract from discharge curves, since both current and voltage decay with time. Information may be more readily obtained from constant-current discharge curves. Recharge may also be

Table II

Some Standard Potentials at 25°C Relative to the Standard Silver Electrode in Acetonitrile [12]

Half-reaction	E°, volts
$Cu^{2+} + e^- \rightarrow Cu^+$	0.679±0.001
$Ag^+ + e^- \rightarrow Ag(Hg)$	0.0870±0.0005
$Ag^+ + e^- \rightarrow Ag$	0.000
Ag^+ (0.0100 M $AgNO_3$) $+ e^- \rightarrow Ag$	-0.131±0.001
$Cu^+ + e^- \rightarrow Cu(Hg)$	-0.5942±0.0005
$Cu^+ + e^- \rightarrow Cu$	-0.6044±0.0005

accomplished by several methods - constant current, stepped constant current, exponential current, constant potential, or some combination of these. Constant current charges are slow if the current is held sufficiently low that the battery can be fully charged. A stepped constant current charge is faster. In this method, a large current is passed until a predetermined state of charge is reached, and charge is completed at a lower current level. Exponential charge rates are fastest, but most difficult to instrument. They place a heavy strain on the charger, and can be used only on batteries that can tolerate heavy initial currents. Constant-potential charges are generally fast, but must usually be modified to limit initial current levels when applied to a fully discharged cell. This modification may readily be accomplished by inserting a series resistor between charger and battery. Because of ohmic drop across the resistor the voltage applied to the cell itself is not constant, but is lower at higher charging currents and approaches the voltage of the charging source asymtopically. Therefore, the term "controlled potential charge" should be used rather than the misleading expression "constant-voltage charge". Discharge methods utilized in the present work were discharge through constant resistance and discharge at constant current. Recharge methods chosen included constant-current recharge, stepped constant-

current recharge, and controlled potential recharge.

In the current investigation, a series of cells involving the copper(II)-(I) and copper(I)-(O) couples in acetonitrile were designed and constructed. Mechanical problems caused by leakage of acetonitrile, which has a low viscosity and surface tension, required many modifications in cell design and in the materials of construction. Ultimately two cells were prepared that showed only slight leakage over a period of weeks, and most of the data reported here are based on measurements of these cells.

II

EXPERIMENTAL

Purification of Acetonitrile

Technical grade acetonitrile (Matheson, Coleman, and Bell) was purified by method D1 described by Coetzee [3], but with some modifications. The commercial product was stirred with CaH_2 (Ventron) at a ratio of 10 g/l. Because no hydrogen evolution was observed, stirring was continued for only three hours instead of the two days recommended by Coetzee. To the decanted liquid P_4O_{10} (British Drug House) was added at a ratio of 5 g/l, and the mixture was distilled in an all-glass still under high reflux ratio. The first 5% and last 20% of the still output were discarded. The resulting material was refluxed over CaH_2 (5 g/l) for one hour, then distilled slowly under a high reflux ratio. Again, the first 5% and last 20% of the still output were discarded. The collected product was placed in a tightly stoppered glass bottle and transferred to a dry box until use. All flasks were oven dried at least two hours at 110° before use. The water content of the solvent was checked by Karl Fischer titration. A value of 5×10^{-4} $\underline{M}$ was obtained.

Other Reagents

The $Cu(ClO_4)_2 \cdot 4CH_3CN$ used was the same lot as

used by Kratochvil and Senne [12], who reported a purity of 99.6% on the basis of analysis for copper by aqueous EDTA titration.

$NaClO_4$ (anhydrous, G. F. Smith) was dried under vacuum for 20 hours, then transferred to a dry box and used immediately.

$LiClO_4 \cdot 3H_2O$ (G. F. Smith), recrystallized from water and vacuum dried by R. A. Long, was heated to 80° under vacuum for one day, then to 100° for two more days. It was transferred to a dry box and stored in a tightly closed oven-dried reagent bottle until use.

All other chemicals were reagent grade and were used as received.

The supporting electrolyte and $Cu(ClO_4)_2$ solutions were prepared in a dry box. A triple-beam balance was used to weigh the reagents into a volumetric flask which was then filled to the mark with purified acetonitrile. The $AgNO_3$ for the reference electrode was weighed externally on an analytical balance, then transferred to a dry box for dissolution. All glassware was oven-dried at 110° before use.

Apparatus

Voltages were measured with a Heath EU-805 Universal Digital Instrument (UDI) and an Orion Model 701 Digital pH Meter. These units were separately calibrated

against a Leeds and Northrup 7554 Type K-4 potentiometer. The controlled-potential charge source was two Burgess #6 1.5 v Heavy-Duty dry cells connected in parallel. A Leeds and Northrup Model 7960 Coulometric Analyzer was used for preliminary constant-current studies. However, because this instrument provides only two current levels in the range of interest, 6.43 ma and 64.3 ma, most of the data on constant-current studies were obtained with a Sargent Model IV Coulometric Current Source. Current-time and voltage-time curves were recorded in either a Heath EUW-20A or an EU-20B chart recorder, both equipped with a Heath EU-20-26 Multi-Speed chart drive, or on a Sargent Model SR recorder. Current-time curves were integrated with an Ott planimeter. Control circuits were breadboarded using a Heath EU-801A Analog-Digital Designer (ADD).

A block diagram of the arrangement for cycling by controlled potential charge and discharge through a constant resistance is shown in Figure la. The circuitry in the Heath ADD is described in the Appendix. It may be considered here as an on-off charge-discharge switch. In this arrangement, the cell is discharged through a constant resistance. As explained earlier, the term "controlled potential charge" is used here to describe a constant voltage source with a resistor in series with

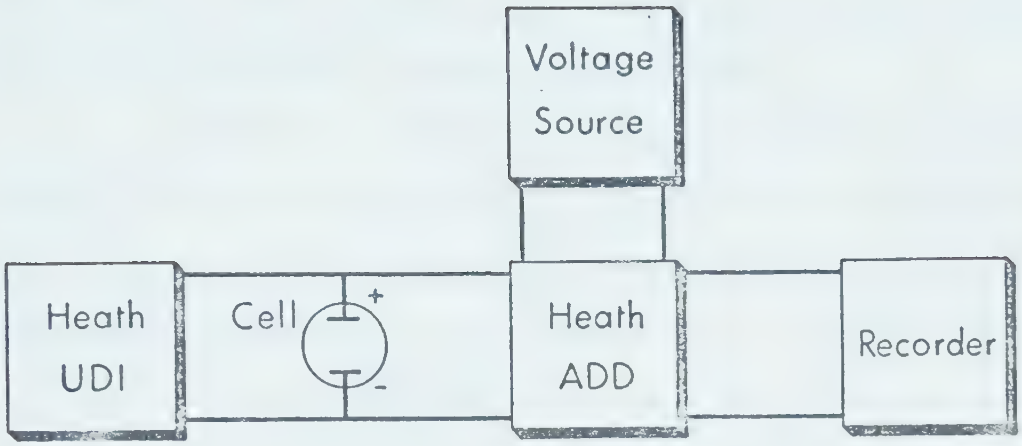

Figure 1a. Experimental Arrangement for Controlled Potential Charge and Discharge Through Constant Resistance.

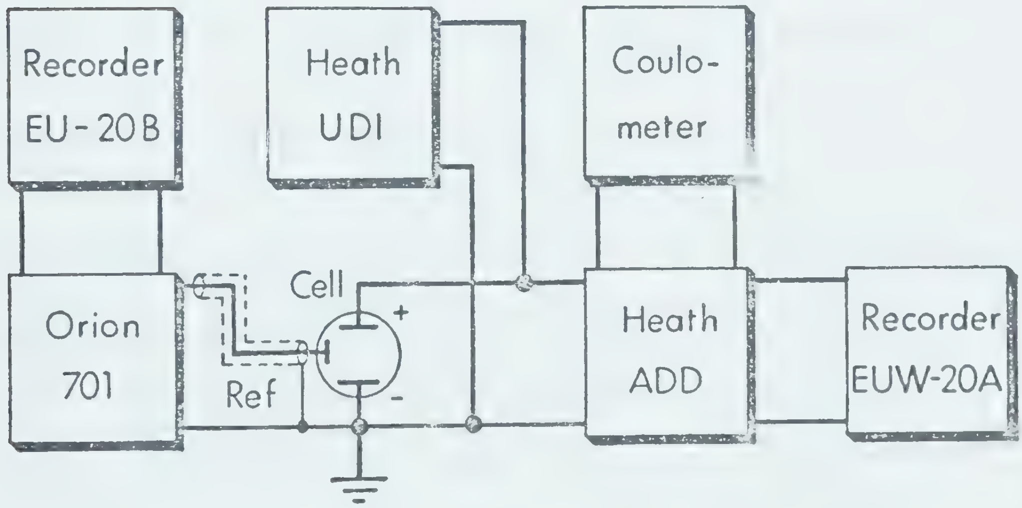

Figure 1b. Experimental Arrangement for Constant Current Charge and Discharge.

the output. The recorder provides a continuous record of charge or discharge current against time.

Figure 1b shows the arrangement for constant current charge and discharge. The control circuitry in the Heath ADD for this system is also described in the Appendix. The overall cell potential is monitored by both the Heath UDI and Heath EUW-20A recorder, while the Orion 701 and Heath EU-20B recorder provide a record of reference electrode potential with respect to the grounded negative terminal. A shielded cable was necessary to connect the reference electrode to the Orion to minimize noise pickup. The Heath EU-20B recorder possesses a floating input, since grounding either of the recorder output terminals of the Orion in this configuration drives it off scale.

Overall Battery Construction

A diagram of the anodic and cathodic sections of the experimental battery is shown in Figure 2. The case was constructed from two identical 10 cm by 10 cm blocks of 1/2 in. (1.27 cm) polyethylene. An 8 cm by 8 cm cavity was milled to a depth of 1 cm in each block. An 8 cm by 8 cm piece of 1/8 in. (0.32 cm) or 1/4 in. (0.63 cm) graphite sheet was press-fitted into one cavity to serve as a cathode. External electrical contact with the graphite was made through a platinum wire press-fitted into a hole drilled through the case into the graphite. Tapered polyethylene tubes tapped with septum

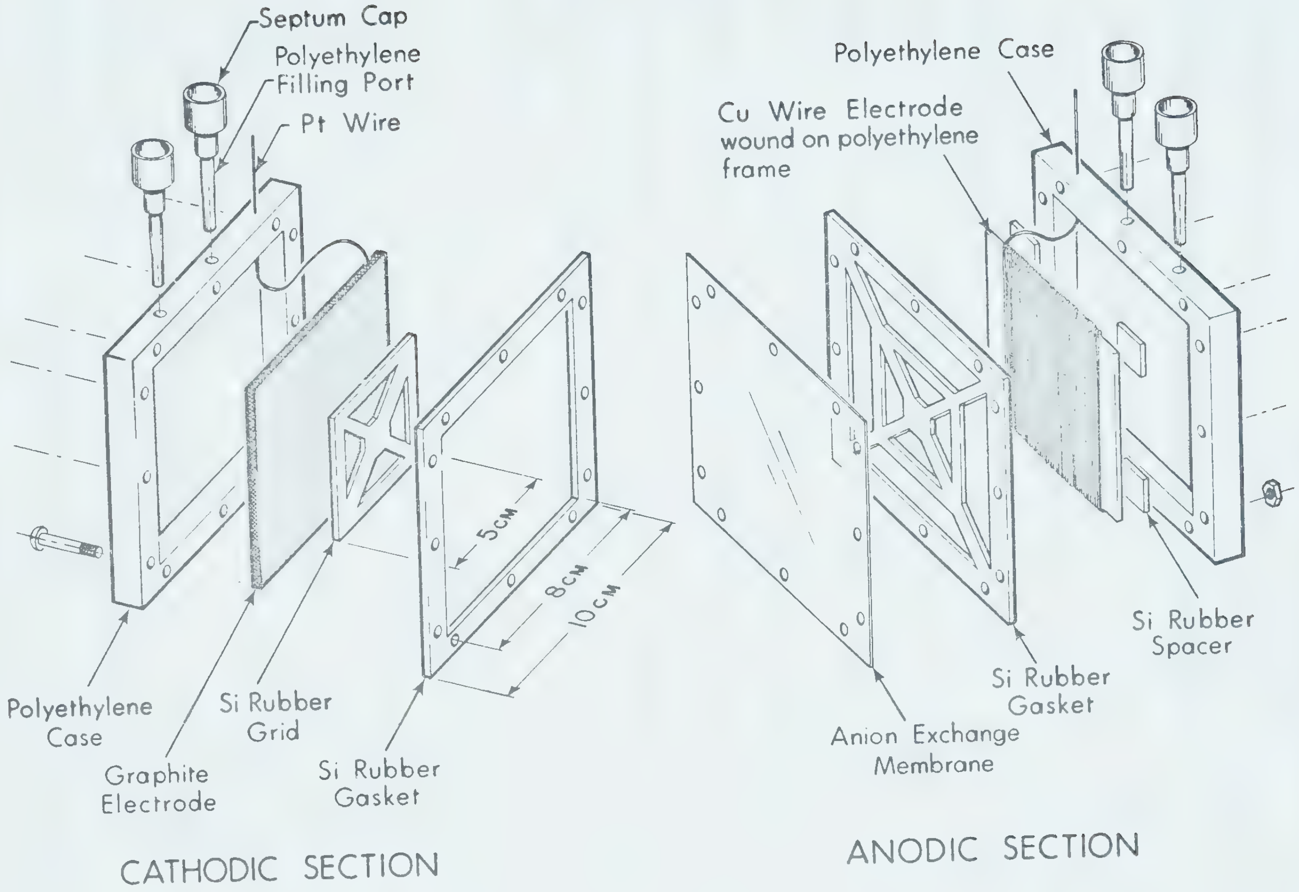

Figure 2. Cathodic and anodic sections of disassembled battery.

caps were sealed into holes drilled into an edge of the chamber to provide filling ports. A 5 cm by 5 cm grid of 1/8 in. (0.32 cm) silicone rubber was bonded to the graphite surfaces by a dot of silicone cement to provide a spacer for the ion-exchange membrane.

An anode, consisting of about fifty feet of 0.032 in. diameter electrolytic copper wire wound on a polyethylene frame, was cemented into the anodic cavity of the case such that solution could freely contact both sides of the electrode assembly. One end of the wire passed through a slightly undersize opening in the polyethylene wall to provide external electrical contact. Filling ports similar to those described for the cathodic section provided a means for addition or removal of solution.

In the assembled cell, a silicone rubber gasket was placed on each side of the membrane to provide a seal with the polyethylene casing. The gasket on the anodic side was bonded to a silicone rubber grid similar to that used on the cathodic side. The cell was held firmly together by twelve bolts spaced on the circumference. Solutions were injected through one of the two filling ports in the appropriate compartment with a syringe; a syringe needle inserted through the septum cap of the other port allowed air to escape.

Anode Preparation

Electrolytic wire (#20) was wound onto a previously weighed polyethylene frame to form the anode. The weight of copper was obtained by difference, and the nominal surface area calculated by the relationship

$$A = \frac{4w}{d\rho} - \pi d \ell_e$$

where w = weight of Cu(g)

d = diameter of wire (cm)

ρ = density of Cu (g/cm^3)

ℓ_e = length of wire outside the anodic chamber (cm)

Geometric surface areas of copper for the two cells were 328 and 401 cm^2 (0.9 and 1.2 moles copper).

The surface of the copper was treated with concentrated HCl for two minutes, then rinsed throughly with distilled water. The assembly was immediately vacuum dried overnight and placed in a dry box for final cell assembly. Visual inspection of the surface immediately before cell assembly did not reveal any traces of a surface film of copper oxide. However, electrodes that were washed with technical grade acetonitrile before vacuum drying developed a shiny coating over their entire surface. Portions of the surface also appeared black or yellow, indicating formation of a surface film.

Cathode Preparation

A different procedure was used for pretreatment of the cathode in each of the cells on which data are primarily based. For Cell 1, the graphite electrode, which had been used in earlier studies, was washed with distilled water and sanded lightly with emery paper before vacuum drying. It was later found that the graphite had adsorbed considerable amounts of copper salt during previous use. Therefore, the graphite electrode for Cell 2, which also had been used before, was immersed in boiling water for several days to extract adsorbed salts. Each electrode was dried under vacuum overnight and then transferred to a dry box for final assembly of the cell.

Membrane Preparation

Table III gives some properties of the Amfion A-60 anion exchange membrane used in this study[22]. The membrane utilizes a polyethylene backbone containing quaternary ammonium exchange sites. A sheet approximately one foot square was converted from the chloride form in which it was received to the perchlorate form by soaking in aqueous 1 $\underline{M}$ $NaClO_4$ for one hour, then stored in a fresh bath of 1 $\underline{M}$ $NaClO_4$ until use (several weeks). When a cell was to be constructed, a portion about 12 cm by 12 cm was cut from the sheet and soaked in technical grade acetonitrile overnight. During this time, the lateral dimensions

Table III

Nominal Properties of Amfion A-60 Anion Exchange Membrane[22]

Thickness, wet (mils)	12
Resistance, effective (0.6 N KCl), ohm-cm^2	6±2
Permselectivity (0.5 N/1.0 N KCl), %	82±4
Ion exchange capacity (dry), meg/g	1.6±0.3
Gel water (dry basis), %	28±5

increased about 10% over the water-wet form, the thickness decreased, and the flexibility increased markedly. The membrane was then removed from the bath and cut to a final size of 10 cm by 10 cm. Bolt holes were punched along the edges, after which the membrane was vacuum dried overnight and transferred to a dry box immediately before final assembly of the cell.

Final Assembly

Immediately upon introduction into the dry box, the membrane was soaked in purified acetonitrile. When it had expanded to maximum size, the cell components were bolted together and the cell compartments immediately filled with previously prepared acetonitrile solutions of copper(II) perchlorate on the cathode side and lithium or sodium perchlorate on the anode side.

Reference Electrode

The reference electrode assembly is shown in Figure 3. The reference couple was Ag-0.0100 $\underline{M}$ $AgNO_3$ in acetonitrile. The electrode was inserted into a $LiClO_4$ solution of the same concentration as the supporting electrolyte in the cell under study. Solution contact was effected through a Luggin capillary of 0.034 in. i.d. polyethylene tubing. A glass bead was inserted in the end of the tubing to minimize solution flow.

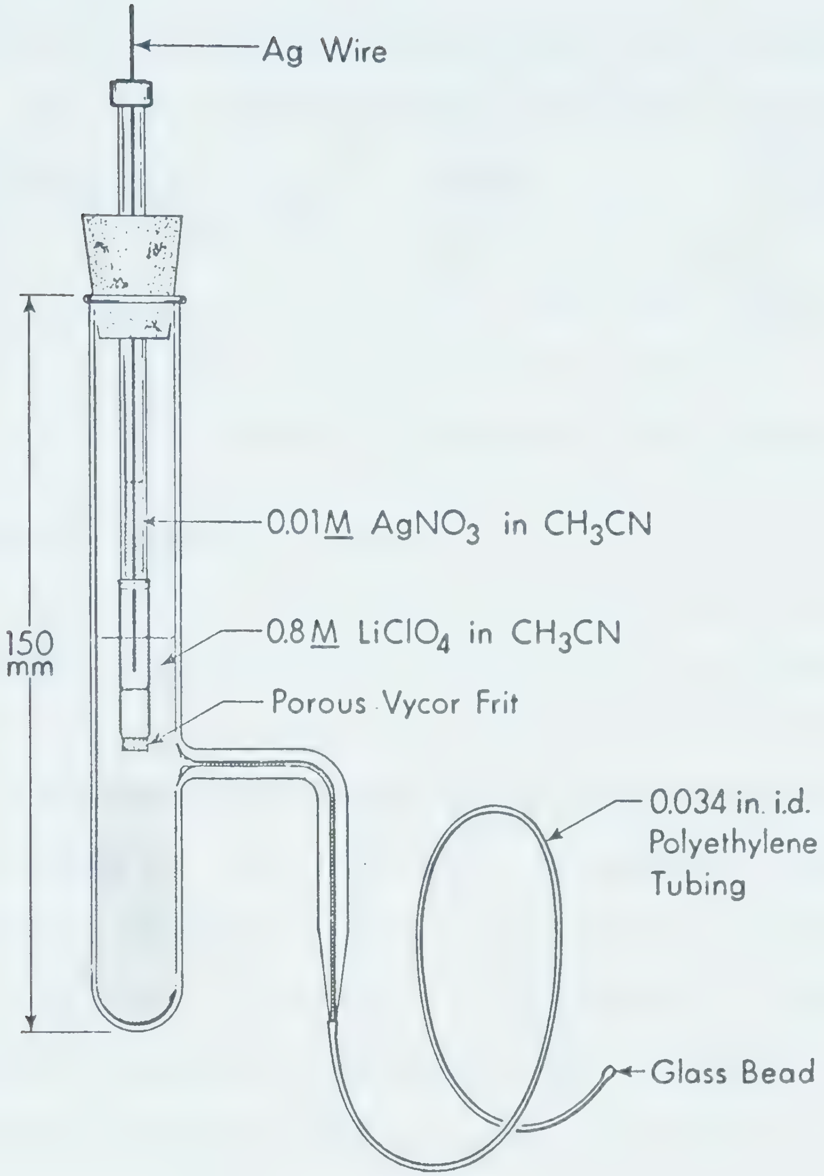

Figure 3. Reference Electrode Assembly.

The capillary was inserted through a septum cap and filling port of one cell compartment and down into the solution. Exact positioning of the capillary end could not be determined owing to the flexibility of the tubing and the opacity of the cell. However, the general location was arranged such that the capillary end was near the vertical centerline of the electrode and about 2 cm from the top of the solution to minimize edge effects.

Initial Specifications of Cells

In Table IV are listed the initial characteristics of the two cells on which most of the data were taken. The actual capacity of Cell 1 is unknown because the graphite electrode contained adsorbed copper salts and because recovery of the solutions on disassembly was not quantitative. The uncertainty of the theoretical capacity of Cell 2 is based on estimates of the errors in measuring the volumes of solutions introduced into the cell. Leakage also resulted in loss of electrolyte, particularly on Cell 1, where introduction of more $NaClO_4$ solution to the anodic compartment at the rate of about 5 ml/month was necessary. Because some cycles took as long as seven days for discharge and recharge, thorough testing required several months.

Table IV

Initial Specifications of Cells

	Cell 1	Cell 2
Total copper metal in anode, moles	0.93	1.151
Nominal anode surface area, cm^2	328	401
Electrolyte	$NaClO_4$	$LiClO_4$
Initial electrolyte concentration, moles/l	0.96	0.896
Initial volume of electrolyte, ml	50	52
Initial electrolyte introduced, moles	0.48±0.005	0 0.047±0.002
Thickness of graphite electrode	1/4 in. (0.63 cm)	1/8 in. (0.32 cm)
Initial concentration of $Cu(ClO_4)_2$ in CH_3CN, moles/l	0.16	0.366
Total volume of $Cu(ClO_4)_2$ solution, ml	30	41
Total $Cu(ClO_4)_2$ introduced, moles	0.0048 *	0.0150±0.008

(Table continued on next page)

Table IV continued

	Cell 1	Cell 2
Theoretical capacity, ma-hr (based on 100% utilization of $Cu(ClO_4)_2$)	129 *	402±20

* It was later found that the graphite electrode contained at least a further 0.005 mole of adsorbed copper salt.

III

RESULTS AND DISCUSSION

Preliminary Investigations

A number of preliminary investigations were conducted outside the dry box. Several cells were constructed utilizing technical grade acetonitrile, with anodes of copper sheet rather than electrolytic copper wire. Performance of these cells was unsatisfactory because of formation of an adherent black resistive film on the anode. Preliminary investigations also suggested that internal resistance was highly dependent on the surface area of the anode. Further, the anion exchange membranes showed severe yellow discoloration, probably from adsorption of copper oxide and hydroxide species formed by reaction of the copper salts with water. Further work was therefore conducted in a dry box, utilizing cells possessing an anode of large surface area. Great care was taken to exclude water from these cells.

Cell Performance Under Discharge Through Constant Resistance and Recharge at Controlled Potential

Cell 1 was subjected to more than 45 cycles of discharge through constant resistance followed by recharge at a controlled potential. Most discharge cycles continued until the cell voltage under load dropped to 0.9 - 1.0 v.

Each discharge was followed by immediate recharge until the charging current dropped to less than 0.5 ma, which was taken to indicate full charge. Figure 4 shows a discharge curve to extreme depth, while Figure 5 shows the immediately following recharge. Discharge voltage is directly proportional to discharge current through Ohm's Law.

Figure 6 shows a plot of milliampere hours drawn on discharge against milliampere hours accepted on subsequent recharge for the first 11 cycles of Cell 1, each varying in depth of discharge. A charge efficiency of 100% would be indicated by a slope of unity and an intercept of zero. A computer least-squares treatment of the data utilizing a program provided by G. Horlick yielded a slope of 1.004 ± 0.021 and an intercept of 2.042 ± 2.062. It must therefore be concluded that coulombic efficiency under conditions of discharge through constant load and controlled potential recharge is close to 100%. These data are consistent with the known reversibility of the copper(II)-(I) and copper(I)-(0) couples in acetonitrile.

No degradation in performance of Cell 1 was noted after more than 45 cycles to varying depths. Instead, the available capacity increased. The second discharge, which was to extreme depth, yielded 180 ma-hr although the expected capacity was only 129 ma-hr based on the amount

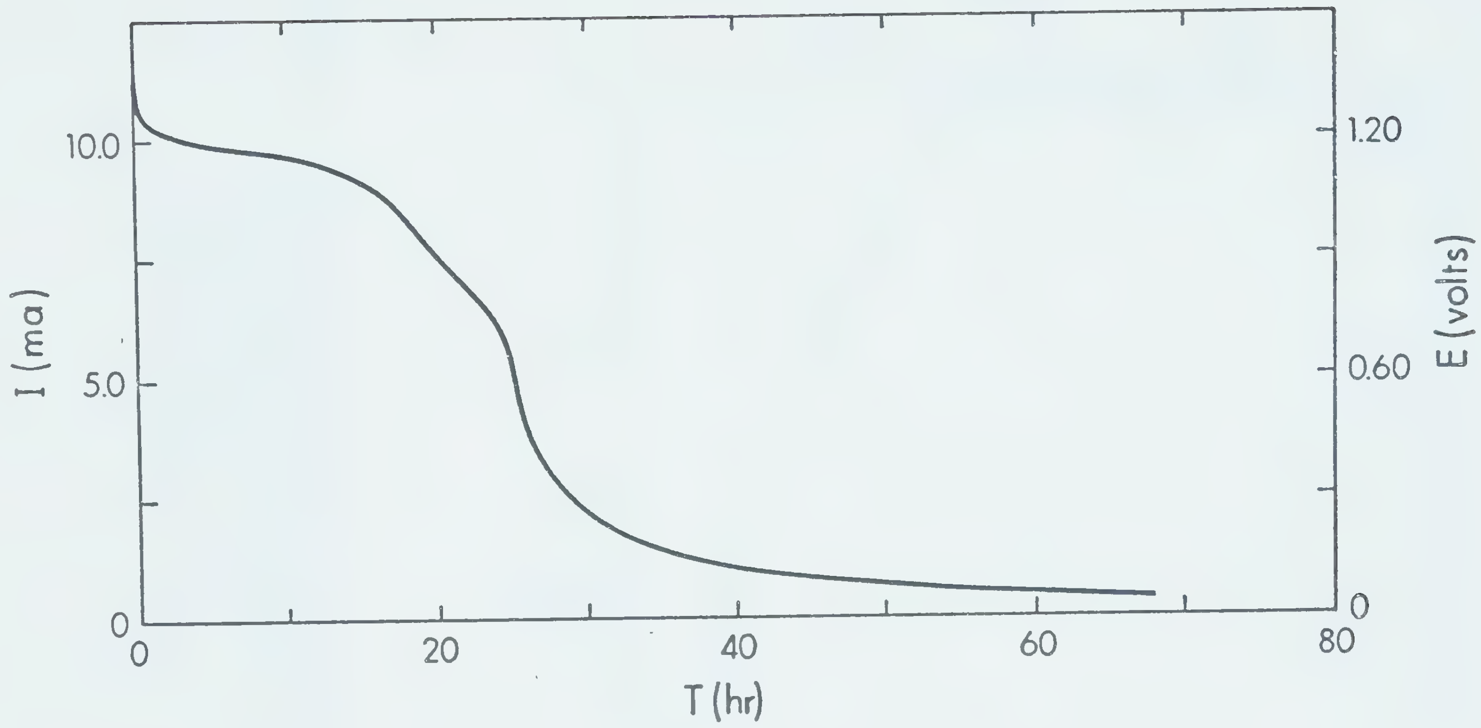

Figure 4. Discharge Through Constant Resistance to Extreme Depth. Cell 1. Load Resistance = 120 ohms.

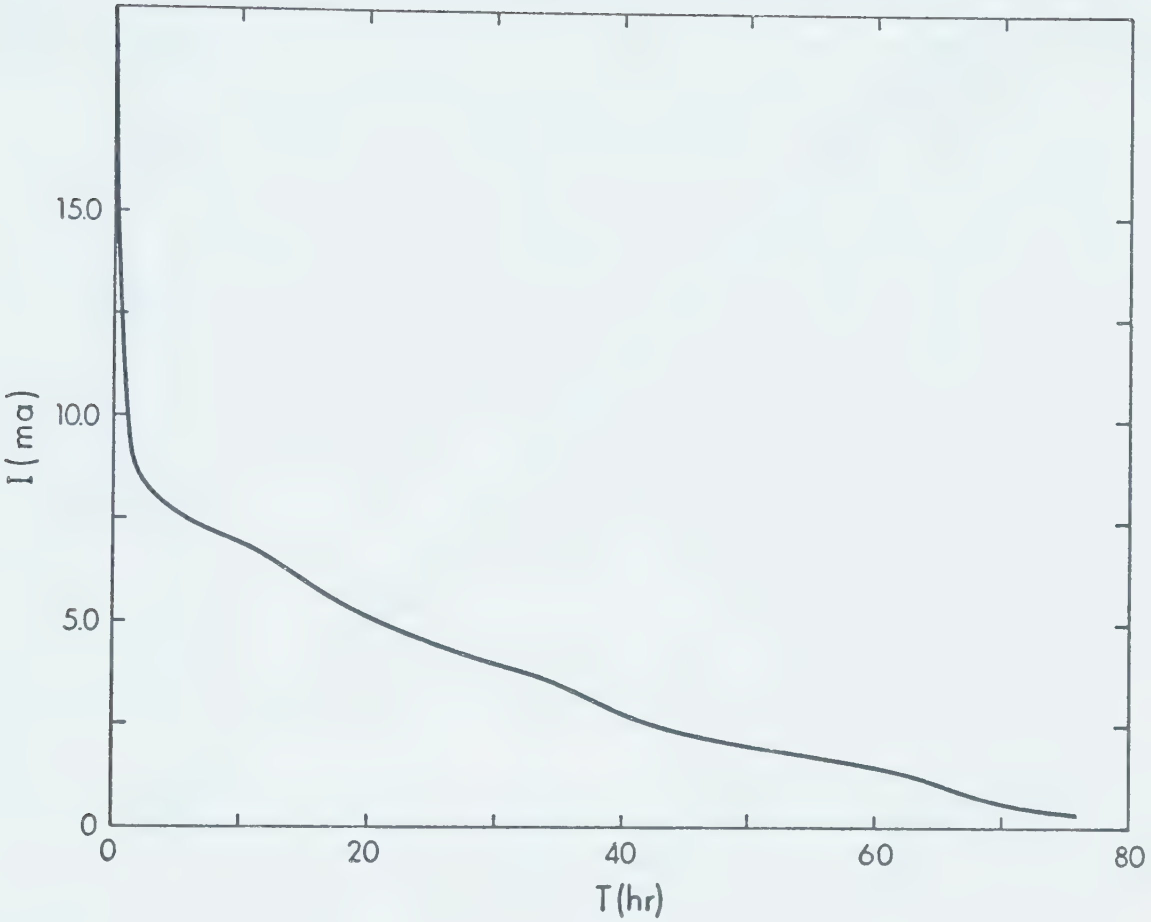

Figure 5. Typical Controlled Potential Recharge Curve.
Cell heavily polarized by discharge at commencement of recharge.
Initial current >35 ma
Charging voltage - 1.5 v.
Series resistance - 20 ohms.

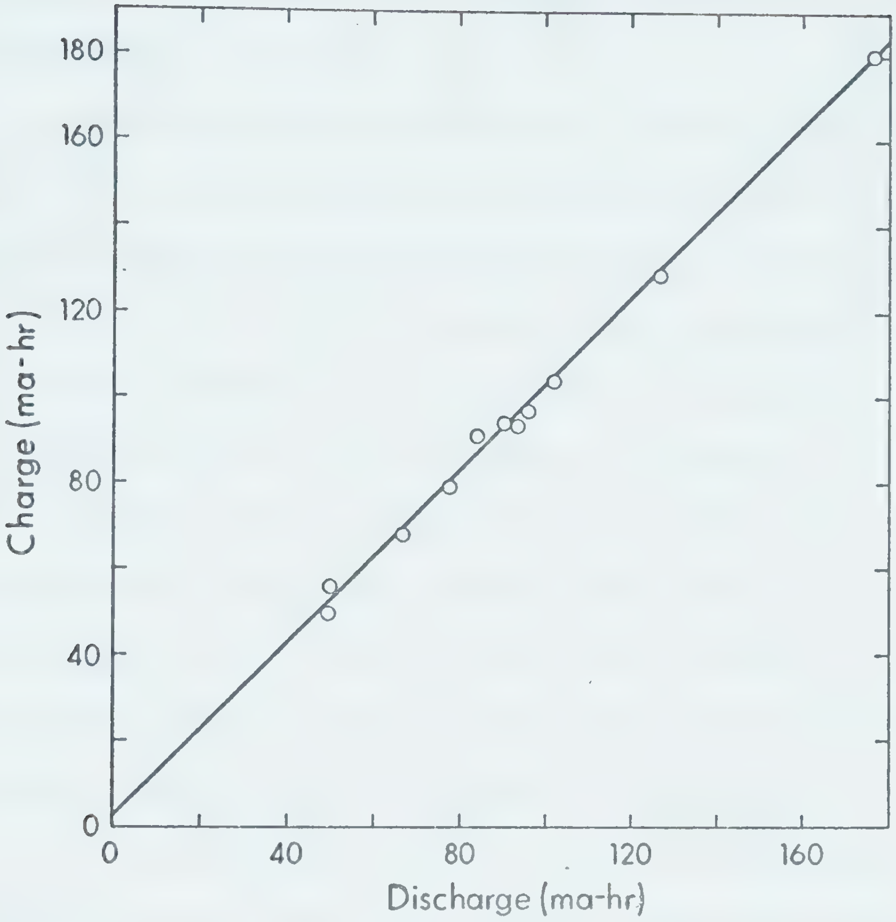

Figure 6. Least Square Fit of Total Charge *vs.* Immediately Preceding Discharge of Cell 1. Discharge through constant resistance and controlled potential recharge.

of $Cu(ClO_4)_2$ introduced at assembly. By the twenty-third cycle, which is shown in Figures 4 and 5, capacity had increased to 267 ma-hr. No further increase was observed upon subsequent cycling.

Quantitative recovery of solutions upon disassembly of the cell after full recharge was not possible. However, analysis of the cathodic solution for total copper by reaction with iodide in aqueous solution and titration of liberated iodine with thiosulfate [23] yielded a result of 0.0071 ± 0.0002 mole present in solution. A further 0.0023 ± 0.0001 mole was obtained by extraction of adsorbed salts from the graphite electrode, yielding a total recovery of 0.0094 ± 0.002 mole copper. A recovery of a minimum of 0.010 mole copper was expected on the basis of maximum discharge capacity obtained.

The increase in the capacity of the cell might be attributed to formation of extra copper(I) species at the cathode, and migration of that copper(I) through the membrane to the anodic compartment where it would be converted to copper(II) during recharge. Such a process requires both a mechanism for the production of the excess copper(I) and a driving force for its transfer across the anion-exchange membrane. However, the conversion of that copper(I) to copper(II) at the graphite electrode during recharge could be expected to appear in a plot of recharge

against discharge as a slope of greater than 100%, indicating low recharge current efficiency. A particularly marked effect should have been observed during the first recharge, since discharge capacity increased 50% between the first and second cycles. However, such a trend was not observed, and Cell 2 did not exhibit a similar increase in capacity. Therefore, it was concluded that the observed increase in the capacity of Cell 1 was not due to an electrochemical process but was caused by extra $Cu(ClO_4)_2$ adsorbed on the graphite electrode. This conclusion is supported by the fact that 0.0023 mole of copper was extracted from the electrode after disassembly.

Cell Performance Under Conditions of Charge and Discharge at Constant Current

Cell 2 was cycled entirely by discharge at constant current and recharge at either constant current or stepped constant current. All discharges were continued to complete discharge as indicated by a final voltage of 0 v. Recharges were continued to a voltage of 1.600 v, which is just below a sharp rise in cell potential caused by the inability of available copper(I) species to support the applied current. On all recharges, after the first termination of the recharge process, the cell was allowed to stand overnight to depolarize. Recharge was then con-

tinued, usually at a lower current level, until acceptance of only a small incremental charge at the lowest current level of 4.65 ma indicated complete charge.

A plot of total recharge against immediately preceding discharge is shown in Figure 7 for 11 discharges of varying depths. A computer least-squares treatment of the data yielded a slope of 0.947 ± 0.022 and an intercept of 9.812 ± 4.554. These calculated parameters suggest a tendency for the cell to undercharge after lengthy drain, but to overcharge after brief drain. These data may be explained by the excessive polarization of the cell that occurs after a lengthy recharge. This polarization causes the voltage across the cell to rise prematurely, resulting in early termination of the recharge process. The difference is made up during brief recharges because reduced polarization then allows a relatively greater recharge.

Three-electrode Studies

All three-electrode studies were conducted on Cell 2. A plot of cell voltage against time is shown in the upper curve of Figure 8 for a constant current discharge at 9.65 ma. On the same graph is shown a plot of the potential difference between cathode and reference electrode against time. The data were obtained with the capillary connection to the reference electrode immersed

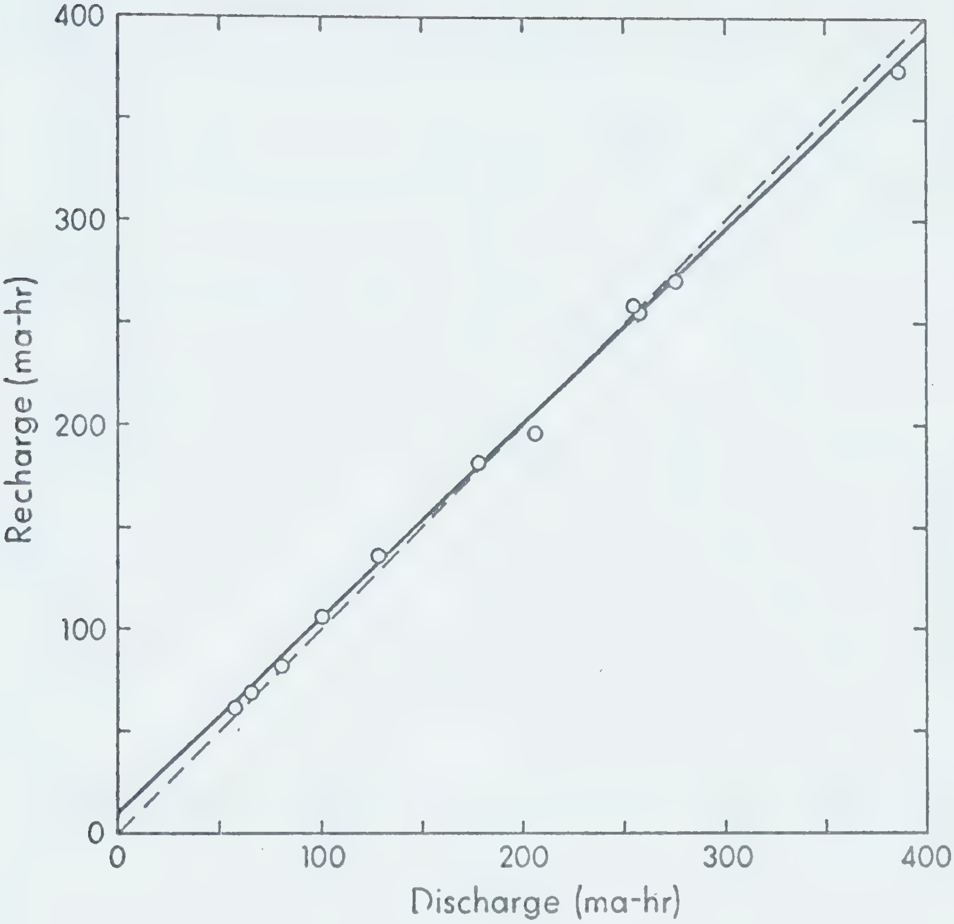

Figure 7. Least Square Fit of Total Charge vs. Immediately Preceding Discharge of Cell 2. Constant Current Cycling. Dotted line represents 100% current efficiency.

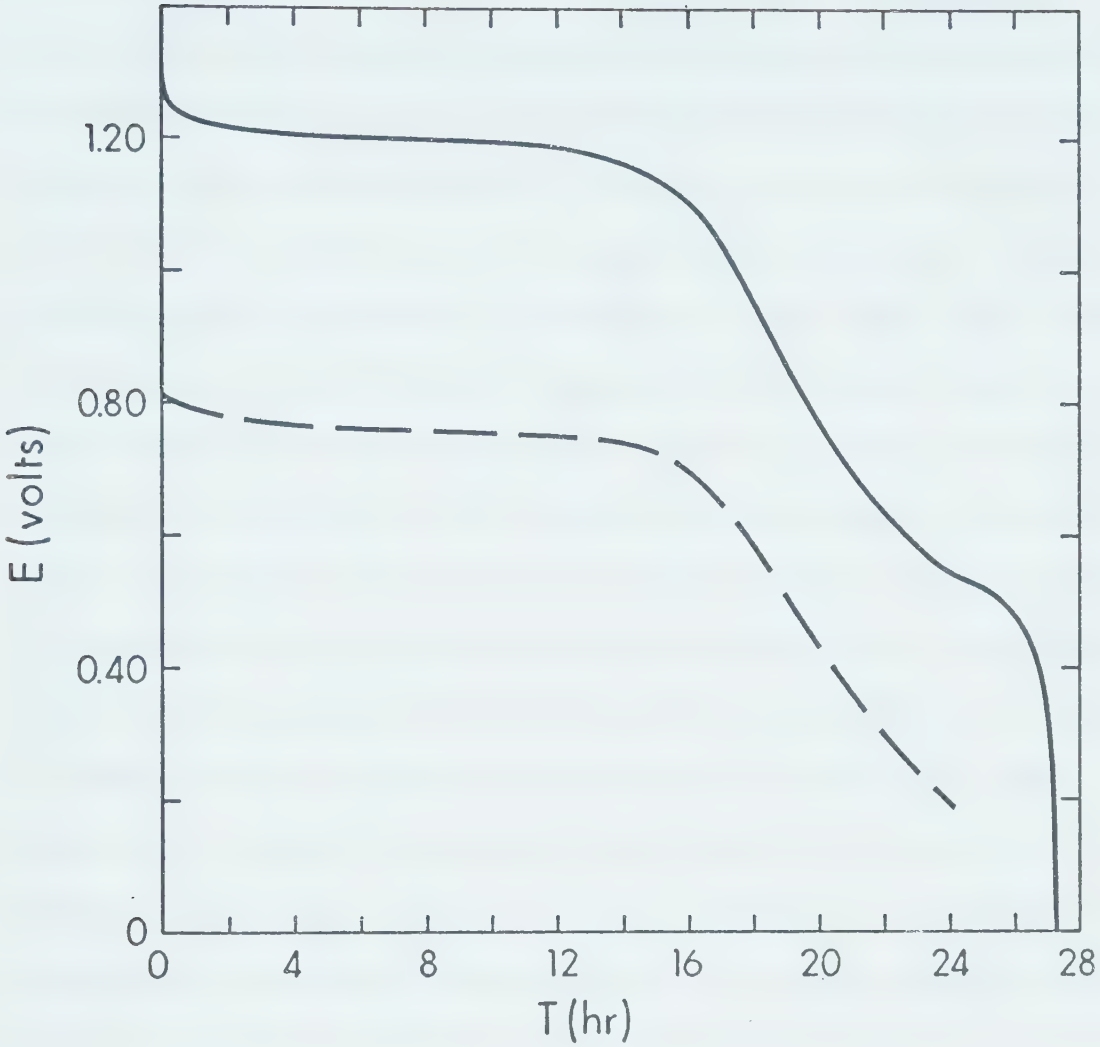

Figure 8. Constant Current Discharge of Cell 2.
I = 9.65 ma
Solid line represents E_{cell}.
Dotted line is difference between cathode and reference potentials.

in the copper(II) solution of the cathode compartment. Therefore, the junction potential between the cathodic solution and the $LiClO_4$ solution in the capillary is included in the measurements. The plot reveals that most polarization occurred at the graphite electrode. Unfortunately, the formation of bubbles in the capillary created a resistance that made it impossible to obtain data for the last part of the discharge. However, data at other levels indicated that the final sharp drop in cell potential was also primarily due to polarization at the cathode. In another discharge at the same current level, but with the capillary immersed in the anodic compartment, a plot of the potential difference between the anode and the reference electrode against time revealed a change of only 0.055 v during the course of the discharge. Recharge behaviour also consistently showed that most polarization occurred at the graphite electrode.

The long shoulder of the discharge curve in Figure 8, which is also visible in the discharge of Cell 1 through constant resistance in Figure 4, did not always appear in other discharge cycles. Preliminary constant current discharges of Cell 1 did not exhibit a shoulder, although discharges through constant resistance did. Further investigation of the electrode processes at the graphite electrode is necessary to determine the reasons

for the erratic behaviour. Adsorption of substances on graphite electrodes often causes irreproducible behaviour, and the presence of traces of foreign substances may be responsible.

Performance Versus Current Drain

The performance of a practical cell depends upon the minimum voltage under load that it can exhibit before it is considered unuseable. Consumer Reports [24], in testing dry-cell battery rechargers, considered that the standard 1.5 volt dry cell was unuseable when its voltage under load had diminished to 0.65 volt. Figure 9 gives the practical discharge capacity in ma-hr that was obtained from Cell 2 at various current levels, the practical capacity being defined as the ma-hr obtained before the voltage under load fell to 0.65 v. Each point represents one discharge from full recharge at a given current level. Although the reproducibility at lower current levels was not good, the plot reveals a rapid drop of practical capacity as current drain increases. The data were obtained under conditions of continuous discharge, so the demand placed upon the battery was considerable. Under conditions of intermittent current drain, with periods during which the cell was allowed time to recover, the practical capacity at higher current levels could be

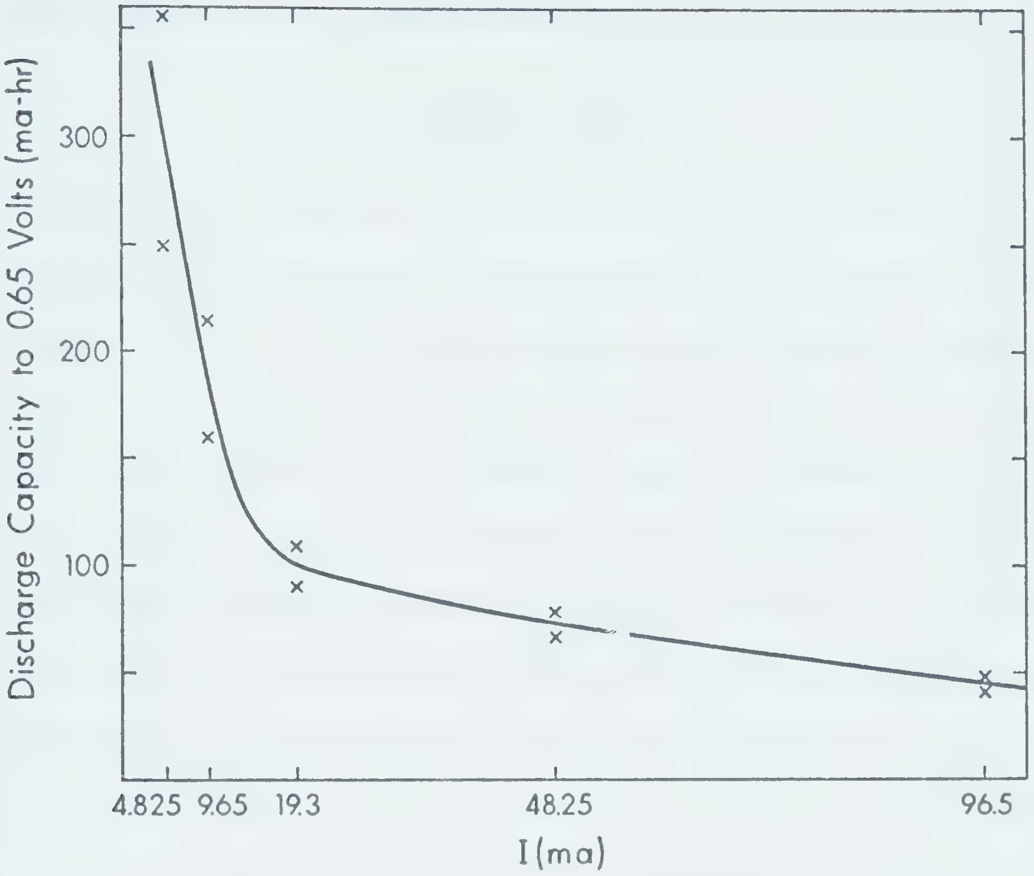

Figure 9. Discharge Capacity to 0.65 volts Under Load. Constant current discharge from full recharge of Cell 2. x's indicate individual points.

expected to be greater than that observed here.

The observed potential, E_{obs}, of a battery under load may be represented as

$$E_{obs} = E_{cell} - IR + \eta$$

where E_{cell} represents the open-circuit voltage, I the current, R the internal resistance of the cell at that current level, and η the overpotential owing to concentration and activation polarization effects. Voltage-time curves at various current levels were extrapolated to zero time to minimize overpotential contributions, and the resulting voltage is plotted against current in Figure 10. Each point is the average of two discharge runs. A computer least-squares treatment of the data yielded an intercept of 1.352 ± 0.007 volts and a slope of 5.11 ± 0.15 ohms.

The intercept yields the practical open-circuit voltage of the cell, 1.35 v. A theoretical open-circuit voltage cannot be calculated because the activity of copper(I) cannot be defined at "full" charge. Freshly constructed or freshly recharged cells exhibit potentials as high as 1.5 v owing to very low copper(I) activity at the electrode surfaces. The potential of these cells is not stable, however, but decreases upon standing. The highest observed potential, 1.50 v following controlled potential recharge of Cell 1 at 1.55 v charging potential,

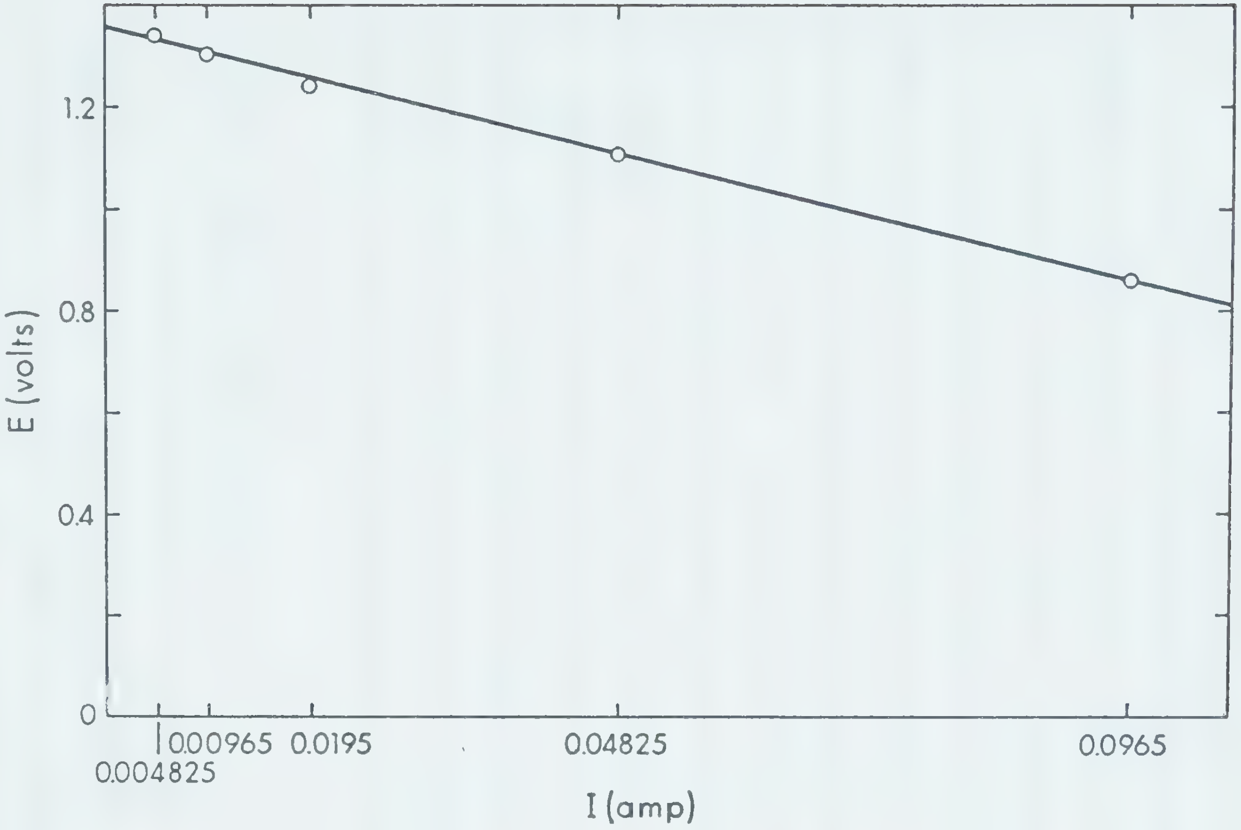

Figure 10. Voltage at Zero Time *vs.* Current.
Each point is the mean of two discharge runs.

decreased to 1.40 v after standing one hour and to 1.36 v after standing four hours. Momentary discharge of a cell with an exceptionally high voltage drops the open-circuit voltage to about the practical level.

The calculated internal resistance of the cell is 5.1 ohms. This is in reasonable agreement with AC impedance measurements, which are illustrated in Figure 11 as a function of state of charge. Impedance should increase as the cell discharges as a result of buildup of solid $CuClO_4$ on both electrode surfaces and as a result of a decrease in the concentration of copper(II) species in the cathode compartment. A general trend of this kind is evident in Figure 11. However, the data were not reproducible, and there was often an upward or downward shift of impedance on standing of as much as one ohm. Impedance measurements at full charge are generally slightly lower than 5.1 ohms, but this difference is probably not significant in view of the uncertainty of the values.

Overall Cycling Performance

Overall performance on repeated cycling appeared to be good. Utilization of electroactive material based on amounts of copper(II) present was as high as 96% on the first discharge of Cell 2, which was run at the lowest current level utilized in these studies, 4.65 ma. Later

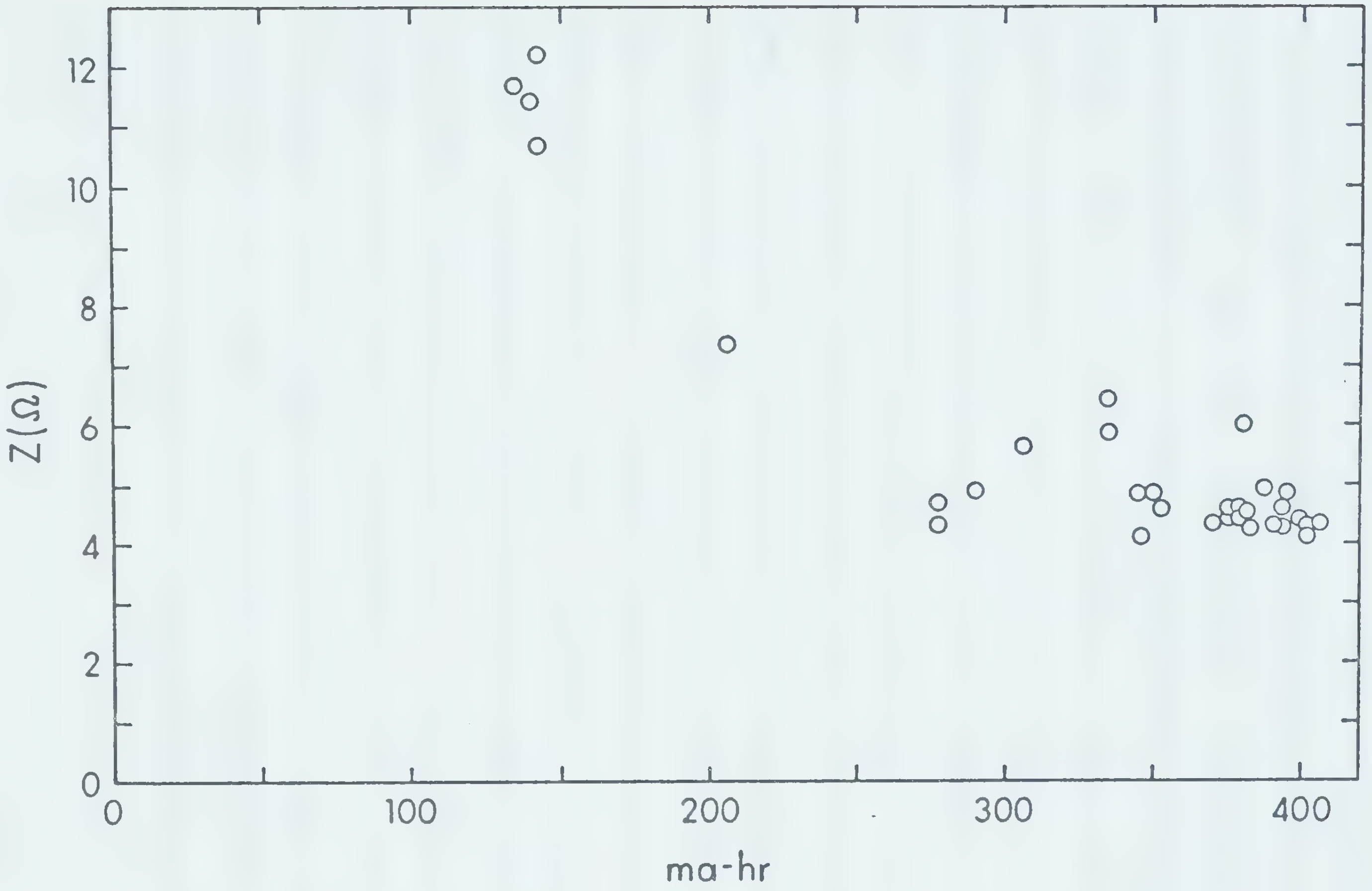

Figure 11. Impedance vs. State of Charge of Cell 2. Full charge ~ 400 ma-hr.

discharges delivered only 65% to 69% of theoretical capacity at low current levels. However, data are insufficient to determine if this reduction in total deliverable capacity is a result of repeated cycling or due to the loss of copper(II) solution by leakage. The total deliverable capacity of Cell 1 decreased 12% after two months wet stand. Full recharge was accepted, indicating that reduction in capacity was not a result of leakage. Wet stand performance thus indicates that Cu^{++} ions do not readily pass through the anion-exchange membrane. This conclusion is supported by the observation that a considerable osmotic pressure head built up in the cathodic compartment of both cells, causing the anion-exchange membrane to distend considerably. Leakage caused solution level to decrease only in the anodic compartment, whereas the cathodic compartment remained completely filled even if the anodic compartment went dry. The exclusion of Cu^{++} by the membrane could be expected to be greater than that of unipositive species because of the higher charge density on the divalent ion, and the only mechanism for self-discharge is the migration of copper(II) species to the anode.

Low-temperature Studies

To obtain a measure of performance at temperatures

below ambient, cell 1 was placed in a vacuum desiccator containing indicating magnesium perchlorate as desiccant and removed from the dry box. External electrical contact was made through wires run through the vacuum takeoff and sealed with silicone cement. The cell and desiccator were then placed in a freezer at -5° and discharged through constant load.

Discharge performance was distinctly below that attainable at room temperature. Discharge through 120 ohms to a final voltage of 0.9 v yielded only 56 ma-hr at -5°, whereas at least 120 ma-hr were attainable at room temperature. Because the cell capacity was increasing during the time that studies were conducted, a quantitative comparison is not possible. However, discharge curves revealed a decrease in cell voltage under load of about 0.075 volts/hour, corresponding to a decrease in current level of about 0.675 ma/hr. This decrease was approximately linear, and was reversed upon removal of the cell from the freezer during the discharge. Behaviour during controlled-potential recharge at low temperature was also significantly below that at room temperature. Initial recharge currents of about 4 ma dropped within two hours to less than 2.5 ma. Only qualitative comparison of these figures with those attainable at room temperature is possible, since current under conditions of controlled-

potential recharge depends heavily on the state of discharge of the cell. However, recharge at -5° was prohibitively slow, and no recharges were completed at that temperature. More than 37 hours was required to recharge a total of 51 ma-hr. An earlier cycle at room temperature was recharged 56 ma-hr in 19 hours. Removal of the cell from the freezer during recharge caused the charging current to double. Low temperature studies of Cell 1 were discontinued when examination of the indicating dessicant revealed moisture pickup.

An attempt was made to conduct low-temperature studies on Cell 2 in the dry box by immersing the cell in a bath of dry ice-ethylene glycol at -14°. After a wait of seven hours to attain thermal equilibrium, a constant current discharge was conducted at a current level of 4.825 ma. Three-electrode measurements were unsuccessful because the bridge solution in the capillary froze. However, the curve of cell voltage against time was similar in shape to those obtained during room temperature studies at low current levels. Deliverable capacity (to 0.65 volts) was 94 ma-hr, compared with deliverable capacities of 356 and 248 ma-hr at the same current level at room temperature. The decrease was probably mainly a result of mass-transport limitations due to increased viscosity of solutions. Plateau voltage, however, was 1.24 v compared with earlier

values of 1.24 and 1.21 v obtained at room temperature at the same current level. Plateau voltages should decrease at low temperatures because of lower cell voltages and higher internal resistance. However, because low temperature discharges are not as deep as those at room temperature, concentration polarization is decreased. Impedance measurements at 1000 Hz indicated an internal resistance of about 20 ohms, four times the impedance measured at room temperature.

Unfortunately, only one discharge could be conducted at -14°. As dry ice was lost through sublimation, the temperature of the bath began to rise and isolated areas of warmth appeared. When more dry ice was added to the bath, it remained on the top of the glycol slurry and chilled the cell, causing a sudden drop in observed voltage. Attempts to force the dry ice to the bottom of the slurry resulted in breakage of the styrofoam container. Further attempts at low-temperature studies were not made.

Observations on Disassembly of the Cells

Disassembly of both Cell 1 and Cell 2 revealed that the copper metal did not redeposit cleanly. A large number of loosely adherent nodules were present, many of which had fallen to the bottom of the compartment and thus could no longer participate in the overall electrode

process. No dentritic growths were observed. Cell 1 did not have a spacer between the membrane and the anode, and the membrane exhibited streaks of discoloring coinciding with individual wires of the metal electrode. These presumably resulted from the membrane being forced against the electrode by osmotic pressure. The membrane of Cell 2 also revealed considerable distention to the anodic side, although the inclusion of a spacer between membrane and anode prevented physical contact and reduced discoloration. The originally colorless, translucent membranes of both cells revealed yellowish and yellowish-greenish discoloration similar to that observed on membranes used in preliminary cells. The copper electrode also showed discoloration, indicating that water had not been completely excluded. The graphite electrodes of both cells were quite clean, with only a few small, white cyrstals adhering to them. Solutions removed from the anode compartment of both Cell 1 and Cell 2 were clear. However, the solution from Cell 1 was blue-green, whereas the solution from Cell 2 had not changed color from the original blue. The solution removed from the cathodic compartment of Cell 1 was a dirty brown and contained many small particiles of copper metal. The cathodic compartment of Cell 2 had gone completely dry at the time of disassembly. These observations indicate that moisture pickup by Cell 1 was

much more serious than that by Cell 2. Much of this pickup probably occurred during the time that Cell 1 was out of the dry box undergoing the low temperature study.

The results of analysis of anodic solutions from Cell 1 for copper content were given earlier. The solution from Cell 2 was analyzed for copper by aqueous EDTA titration by the procedure of Kratochvil and Quirk [25]. To determine the amount of copper that had permeated into the graphite, an extraction procedure similar to that described earlier was used. The electrode was immersed for several days in hot concentrated nitric acid solution. The liquid was decanted and replaced with deionized water. This water was replaced several times. The resulting solutions were combined and concentrated by evaporation. Aliquots of the final solution were also analyzed by aqueous EDTA titration [25]. It was found that the solution obtained from the graphite electrode contained significant amounts of iron. Therefore, aliquots of this solution were adjusted to pH 6 with ammonia and filtered before final adjustment to pH 7.5 for titration. A total of 0.0116 ± 0.0001 mole of copper was found, compared with 0.0150 ± 0.008 mole introduced. The differential may be attributed partly to leakage during testing and partly to spillage during disassembly. Quantitative removal of solutions during disassembly was not possible.

Only 0.00045 ± 0.00007 mole of copper(II) was extracted from the graphite electrode of Cell 2, compared with 0.00227 ± 0.00010 mole extracted from the graphite electrode of Cell 1. The amount of copper salt extracted from Cell 1 is also less than the amount that must have been originally present to explain the observed capacity. However, analysis of the solution removed from the cathodic compartment of Cell 1 revealed more free copper(II) than had been originally introduced. These data indicate that the graphite does not adsorb salts during immersion in acetonitrile, and that salts already present will be released into solution.

Aliquots of the anodic solution of Cell 2 were evaporated to dryness and analyzed for chloride by Fajans titration. Results indicated less than 0.0005 mole Cl^- from a total amount of originally introduced ClO_4^- (as $Cu(ClO_4)_2$) of 0.0300 mole. This indicates that the perchlorate anion is stable towards reduction to chloride under the conditions of charge and discharge used in this study.

The poor quality of the copper metal deposited upon recharge is a drawback, because the loss of copper during plating limits the number of cycles to which the cell can be submitted. Provision of a large excess of copper metal in the cell upon construction would increase

the cycle life, but at the expense of added weight and cost. It is possible that plate characteristics would be improved if an AC component were superimposed on the DC charge. Such asymmetric charging methods have been found to increase physical plate characteristics in other cells [26]. No data are available on the electrodeposition of copper from acetonitrile solution. It may be that agents could be added to the solution that would improve the deposition characteristics.

Comparison with Other Batteries

Jasinsky [27] has devised a figure of merit for a battery of the form

$$M_W = Q_o \varepsilon_I \varepsilon_V K_2$$

where

M_W = observed energy density (W-hr/lb)

Q_o = theoretical energy density (W-hr/lb)

ε_I = current efficiency

ε_V = voltage efficiency

K_2 = weight efficiency

Q_o and K_2 are constants for a given battery, and are defined by

$$Q_o = \frac{F_o E_o}{w_o}$$

$$K_2 = \frac{w_o}{W}$$

where

F_o = theoretical Faradaic capacity of battery assuming 100% utilization of the limiting electroactive component (A-hr)

E = open-circuit voltage of battery (volts)

w_o = weight of redox couples (lb)

W = total weight of battery including solvent, case, separators, etc. (lb)

The observed energy density M_w and the current and voltage efficiency terms E_I and E_V are dependent upon the size of the battery and the rate and depth of discharge. They may, however, be readily calculated for a given discharge at constant current utilizing the relationships

$$M_w = \frac{I \int_o^T Edt}{W}$$

$$\varepsilon_I = \frac{IT}{F_o}$$

$$\varepsilon_V = \frac{\frac{1}{T} \int_o^T Edt}{E_o}$$

where

I = current level (amp)
T = discharge time (hr)
E = observed voltage (v)

In Table V are presented data for three commercial batteries at room temperature [28]. Also presented are data at room temperature and at -14° for the copper-acetonitrile battery studied here. Data for the commercial systems are for deep discharge at a 20 hr rate. Data for the experimental system at room temperature are averages obtained from two discharges at 9.65 ma to 0.65 volts (19 hr). Data for the experimental system at -14° are based on one discharge at 4.825 ma to 0.65 volts (19.8 hr). A value of 1.35 volts was used for E_o of the experimental cell, and Q_o is based on copper and pure $Cu(ClO_4)_2$, rather than the tetrakis-acetonitrile product.

The experimental system has a very low energy density, primarily because of the low weight efficiency K_2. A commercial cell could be expected to possess a much higher weight efficiency. Comparison with the commercial systems listed indicates that a K_2 of 0.4 might be attainable. The observed energy density would then be increased to 8 W-hr/lb at room temperature, even with no improvement in ε_I or ε_V. However, an energy density comparable even with that of the conventional lead-acid cell at room

Table V

Battery Efficiencies

Battery	ε_I	ε_V	K_2	M_w (W-hr/lb)	Q_o (W-hr/lb)
Pb/PbO_2	0.35	0.96	0.41	14.7	112
Cd/NiO	0.39	0.925	0.39	15	107
Zn/Ag_2O	0.75	0.766	0.45	66.1	254
$Cu/Cu(ClO_4)_2$, 25°	0.46	0.85	0.011	0.22	50
$Cu/Cu(ClO_4)_2$, -14°	0.24	0.86	0.011	0.11	50

temperature seems unattainable, owing to the low Q_o of the experimental system. This low theoretical energy density is due to the high equivalent weight of $Cu(ClO_4)_2$, 262, and to the relatively low voltage produced by the cell, 1.3 v.

Data at -14° indicate that the practical energy density of the experimental system is about half that at room temperature. The decrease may be attributed to the reduction in current efficiency ε_I. Neither the lead-acid nor the nickel-cadmium cell exhibits such a marked drop in energy density when temperature is decreased to -14° [29]. The performance of the experimental battery is discouraging in this respect.

Summary

A secondary cell consisting of the copper(II)-(I) and (I)-(O) couples in acetonitrile is reversible, and is capable of repeated cycling. Reproducibility is not great, although the studies were complicated by mechanical difficulties, especially leakage of solutions. Polarization at the graphite cathode is appreciable, although overall voltage efficiency is reasonably high.

Low-temperature studies were complicated by difficulties with water contamination outside the dry box, and with temperature control within the dry box. However,

they indicate that cell performance is appreciably diminished at lower temperatures. The use of an anionic ion-exchange membrane as a separator provides low resistance to current flow. It is stable to the solvent, chemicals, and potentials used, and effectively blocks transport of copper(II) species. Electrodeposited copper metal is loosely adherent under the conditions used, and is poor in quality. The energy density of the experimental system is low, primarily due to the weight of structural components such as case and bolts. However, the relatively low cell voltage and the high equivalent weight of the copper(II) perchlorate limit the maximum attainable energy density.

BIBLIOGRAPHY

1. B. Kratochvil, Crit. Rev. Anal. Chem., 1, 415 (1971).
2. B. Kratochvil, Rec. Chem. Prog., 27, 253 (1966).
3. J. F. Coetzee, G. P. Cunningham, D. K. McGuire, and G. R. Padmanabhan, Anal. Chem., 34, 1139 (1962).
4. F. A. Patty, Ed., "Industrial Hygiene and Toxicology", Vol. II, 2nd. ed., Interscience Publishers, Inc., New York, N.Y., 1967, pp. 2013-16.
5. G. Lago *et al.*, Final Report, Contract DA-36-039-SC-76994 (March 1959)(PB 143899).
6. M. Arcand, Final Report, Contract DA-36-039-SC-72363 (July 1957)(PB 135749).
7. F. Solomon, Proc. Ann. Battery Research Develop. Conf., 12th, Fort Marmouth 1958, 94-8.
8. Manny Shaw, O. A. Paez, and Frank A. Ludwig, Report NASA·Cr-1434, Contract NAS 3-8509 (N69-36829)(Sept. 1969).
9. J. Farrer, R. Keller, and M. M. Nicholson, Final Report, Contract DA-36-039-AMC-03201 (E) (AD 622 818) (1 July 1963 to 30 June 1965).
10. B. Kratochvil and H. L. Yeager, Topics in Current Chemistry, 27, 1 (1972).
11. John K. Senne and Byron Kratochvil, Anal. Chem., 43, 79 (1971).

12. John K. Senne and Byron Kratochvil, *Anal. Chem.*, *44*, 585 (1972).

13. J. M. Kolthoff and J. F. Coetzee, *J. Amer. Chem. Soc.*, *79*, 1852 (1957).

14. Stanley E. Manahan, *Can. Jour. Chem.*, *45*, 2451-2 (1967).

15. Thomas A. Kowalski and Peter James Lingane, *J. Electroanal. Chem.*, *31*, 1-7 (1971).

16. B. McDuffie, private communication.

17. S. G. Biallozer, *Electrochim. Acta*, *17*, 1243-9 (1972).

18. R. Jasinski, "High Energy Batteries", Plenum Press, New York (1967), p. 262.

19. Reference 18, p. 128.

20. J. N. Butler, *J. Electroanal. Chem.*, *14*, 89 (1967).

21. J. Courtot-Coupez and M. L'Her, *Bull. Soc. Chim. Fr.*, *1970*, 1631.

22. "Amfion Ion-Permeable Membranes". American Machine and Foundry Company, Springdale, Connecticut (1964) (commercial publication).

23. W. E. Harris and B. Kratochvil, "Chemical Analysis: An Intensive Introduction to Modern Analysis", Barnes and Noble, Inc., New York (1970), pp. 78-82.

24. *Consumer Reports*, *37*, 755 (1972).

25. B. Kratochvil and P. Quirk, *Anal. Chem.*, *42*, 492 (1970).

26. Reference 18, pp. 263-265.

27. Reference 18, p. viii.

28. Reference 18, p. 47.

29. Reference 18, p. 181.

30. H. V. Malmstadt and C. G. Enke, "Digital Electronics for Scientists", W. A. Benjamin, Inc., New York (1969).

31. Mylène Bréant, Monique Bazouin, Claude Buisson, Monique Dupin, and Jean-Marie Rebattu, Bull. Soc. Chim. Fr., 1968, 5065-72 (1968).

APPENDIX

Circuitry

The circuit used for controlled-potential charging and discharging through constant resistance of the cell is shown in Figure 12. The circuit is drawn in its rest state, that is, with no signal present at the "coil" of any of the relays. In this condition, S_1 is open and the cell is not connected to the charge-discharge circuitry. This feature prevents unrecorded charging or discharging in case of power interruption. When S_1 is closed, a +1.5 volt charging potential is applied to the positive cell terminal and through the series resistance R_s (normally 20 ohms) to ground. R_s provides negative feedback on charging to limit the initial current into a heavily discharged cell. Because of the voltage drop across R_s, the voltage applied across the cell is at a minimum at the beginning of the charge cycle and increases as the state of charge increases and charging current decreases.

In the discharge mode, a logical 1 is present at the $\overline{Q}$ output of the flip-flop (FF). This closes relays S_2 through S_5, and the discharge path is through the series combination of R_D (generally 100 ohms) and R_s. During both charge and discharge, the current flow through R_s

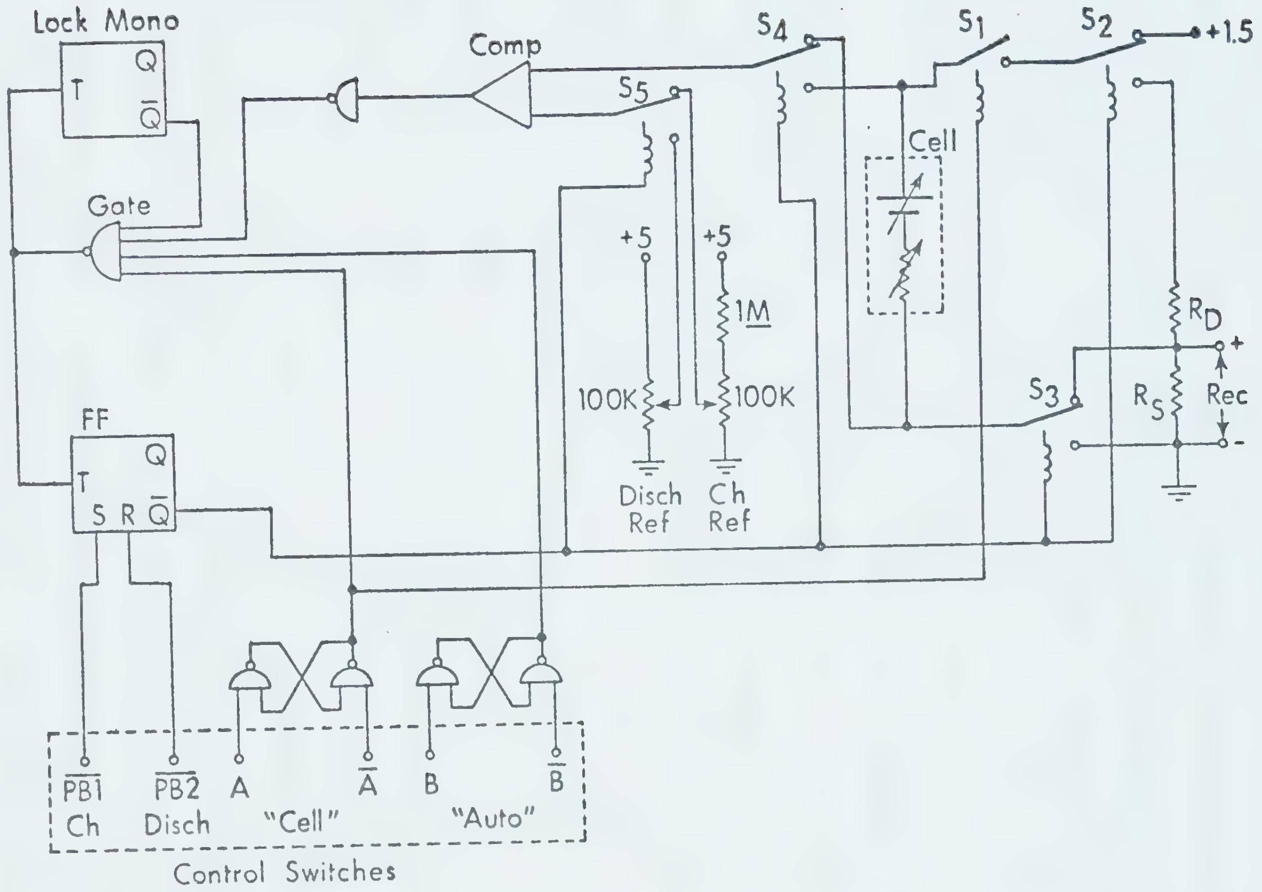

Figure 12. Circuit for Automatic Cycling at Controlled Potential Recharge and Discharge Through Constant Load.

is in the same direction. Connection of a recorder across R_s provides a record of current vs. time. Since the load on discharge is constant, by Ohm's Law the discharge current at any time is directly proportional to the voltage. The negative cell terminal is grounded on discharge, but not on charge. Therefore, direct measurements of cell potential during charge must be made with a voltmeter that will accept a floating input.

Digital circuitry of the type employed here provides a means of automatic switching back and forth between charge and discharge. For switching to occur, a logical 1 must be present both from A("cell") and from B("auto") to unlock the gate. A and B are both panel switches that have been provided with bounce eliminators to prevent spurious pulses from appearing at the gate output. The comparator is an analog-to-digital converter that provides a logical 1 if the voltage present at the input (from S_4) is greater than the reference voltage (from S_5). Separate variable resistances allow adjustment of charge and discharge reference levels. On charge, the comparator monitors the IR drop across R_s. When this falls beneath the reference level, the comparator output goes from 1 to 0; this change is inverted and presented to the gate. Since all other gate input levels are 1, a 1 → 0 transition appears at the gate output and toggles

both the flip-flop (FF) and the lock monostable. Toggling the flip-flop causes S_2 through S_5 to change to discharge mode. The lock monostable provides a momentary 0 at the gate input, thus locking the output at 1 and preventing spurious pulses from the comparator from appearing at the flip-flop input. Similarly, during discharge the overall cell potential is monitored. When it drops below the discharge reference level a 1 → 0 transition again occurs at the gate output and the circuit cycles back to charge. If automatic cycling is not desired, switch B("auto") is set to 0 and the operation must be terminated manually. Push buttons $\overline{PB1}$ and $\overline{PB2}$ provide momentary 0's to manually set charge or discharge mode.

Figure 13 is a diagram of the circuit for semi-automatic constant current charge-discharge cycling of the cell. With no signal present at the coil of any of the relays, S_1 is open and the cell is not connected to the coulometer ("coul"). The potential across the cell is monitored by the recorder through the voltage divider provided by the 90K, two 4.7K, and 1K fixed resistors. The resistors are chosen so that the recorder monitors approximately 5/100 of the cell voltage. Final trim is adjusted with the 1K variable resistance. When a logical 1 is present at C("cell") and the flip-flop is set by a momentary 0 at $\overline{PB1}$, S_1 is closed and current is switched from

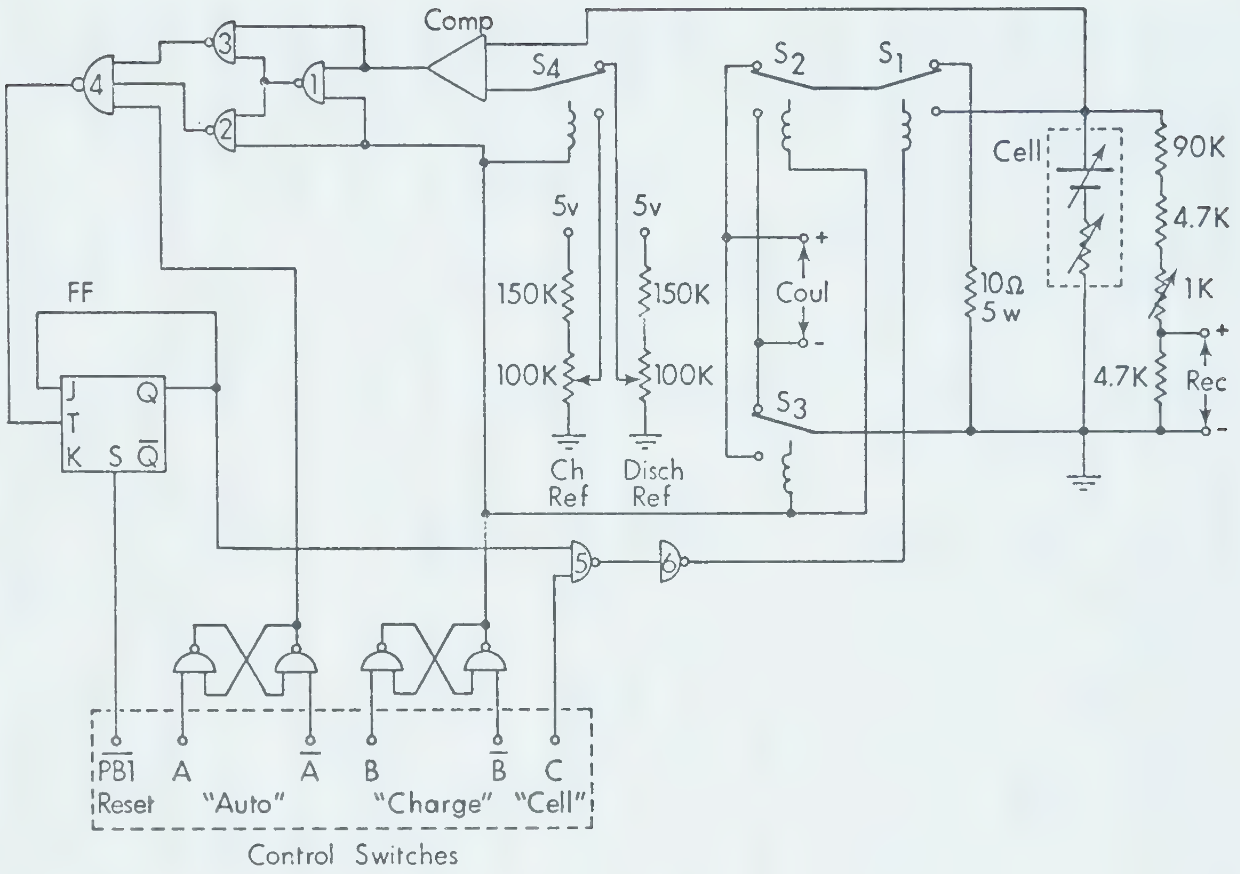

Figure 13. Circuit for Semi-Automatic Charge-Discharge Cycling at Constant Current.

the dummy cell resistor to the cell. With S_2 and S_3 open as shown, the coulometer acts as a current sink and the cell discharges. When S_2 and S_3 are closed, the coulometer leads are reversed and the cell charges. The digital logic provides an automatic shut-off facility when a logical 1 is present at A("auto"). The comparator provides a logical 1 when the cell voltage is less than the reference voltage. Gates 1, 2, 3, and 4 operate as an EXCLUSIVE-OR when A is 1; if A is 0, the output gate is locked in the 1 state.

During charge (B = 1) the cell voltage is normally less than the charge reference voltage and the output of Gate 4 is a logical 1. When the cell voltage becomes greater than the charge reference voltage, the comparator output undergoes a $0 \rightarrow 1$ transition. The output of Gate 4 therefore undergoes a $1 \rightarrow 0$ transition, which toggles the flip-flop. This produces a 0 at the input of Gate 5, allowing S_1 to open and diverting the current into the dummy cell. The connection of Q to J on the flip-flop inhibits any further toggling. Similarly, when the circuit is reset to the discharge mode (B = 0), a $1 \rightarrow 0$ transition at the output of Gate 4 occurs when the cell voltage falls below the discharge reference level. This again causes diversion of current into the dummy cell. Although both the Leeds and Northrup and

Sargent coulometers have provision for external relay control, the circuit shown was more convenient since no special interfacing was needed. In practice, automatic shut-off was rarely used, but was included as a safety facility to ensure that the voltage across the cell did not exceed permissible limits.

A more complete discussion of the individual circuit components may be found in Reference 30.